The right atrium in acromegaly—a three-dimensional speckle-tracking echocardiographic analysis from the MAGYAR-Path Study

Árpád Kormányos[1], Anita Kalapos[1], Péter Domsik[1], Nándor Gyenes[1], Nóra Ambrus[1], Zsuzsanna Valkusz[2], Csaba Lengyel[2], Attila Nemes[1]

[1]2nd Department of Medicine and Cardiology Centre, Medical Faculty, Albert Szent-Györgyi Clinical Center, University of Szeged, Szeged, Hungary; [2]1st Department of Medicine, Medical Faculty, Albert Szent-Györgyi Clinical Center, University of Szeged, Szeged, Hungary

Correspondence to: Attila Nemes, MD, PhD, DSc, FESC. 2nd Department of Medicine and Cardiology Center, Medical Faculty, Albert Szent-Györgyi Clinical Center, University of Szeged, H-6725 Szeged, Semmelweis street 8, P.O. Box 427, Hungary. Email: nemes.attila@med.u-szeged.hu.

Background: Acromegaly is a chronic, rare hormonal disease associated with major cardiovascular co-morbidities. The disease, in the majority of the cases, is caused by a benign human growth hormone (hGH) secreting adenoma. Cardiovascular involvement is especially common in acromegalic patients from the most common hypertension to cardiomyopathy. Left ventricular hypertrophy and myocardial fibrosis are considered common findings in acromegalic cardiomyopathy, which might result in severe heart failure at end-stages. It was set out to quantify right atrial (RA) morphology and function in a group of acromegalic patients using three-dimensional (3D) speckle-tracking echocardiography (3DSTE).

Methods: The study comprised 30 patients from which 8 patients were excluded due to inadequate image quality. Mean age of the remaining acromegaly patients were 53.7±14.5 years (7 males). In the control group 44 healthy adults were enrolled (mean age: 50.7±12.6 years, 15 males). In each case, complete two-dimensional Doppler echocardiography was performed followed by 3DSTE.

Results: All three RA volumetric parameters (Vmax, Vmin, VpreA) were significantly higher in case of acromegaly compared to the healthy controls. Strain analysis revealed that RA function may be enhanced in acromegalic patients, which is more notable in case of active acromegaly. Numerous independent strain parameters had significant correlations with different hormonal variables in the active acromegaly group. These correlations were not present in the inactive acromegaly subgroup.

Conclusions: Acromegaly has a profound effect on RA function and with proper treatment these changes partly seem to be reversible.

Keywords: Right atrium (RA); echocardiography; speckle tracking; three-dimensional

Introduction

Acromegaly is a chronic, rare hormonal disease associated with major cardiovascular co-morbidities, and it is caused by a benign human growth hormone (hGH) secreting adenoma in the majority of the cases (1). High serum levels of hGH entail elevated insulin-like growth factor-1 (IGF-1) serum concentration thus causing a wide range of clinical symptoms and co-morbidities (2). The most important ones are cardiovascular changes including left ventricular (LV) hypertrophy, hypertension (HT), serious valvular regurgitations and LV systolic and diastolic dysfunction at the end-stage disease. The proper mechanism of these changes are not clearly understood currently, it seems that acromegaly at end-stages results in a severe, specific type

of cardiomyopathy due to extracellular collagen deposition entailing myocardial fibrosis (3-5).

Three-dimensional speckle-tracking echocardiography (3DSTE) offers clinicians a new, robust, non-invasive tool for chamber quantification and functional assessment (6). Through strain imaging, 3DSTE is capable of simultaneous and accurate measurement of several global and segmental strain values (7-11). To the best of the authors knowledge, the right atrium (RA) has not been examined before in acromegaly using speckle-tracking methodology. Therefore, it was set out to quantify RA morphology and function in a group of acromegalic patients using 3DSTE.

Methods

Patient population

The study comprised 30 patients from which 8 patients were excluded due to inadequate image quality. Mean age of the remaining 22 acromegaly patients were 53.7±14.5 years (7 males). In the control group 44 healthy adults were enrolled (mean age: 50.7±12.6 years, 15 males). The acromegaly diagnosis was based on the current accepted standards: typical clinical features, elevated hGH levels and elevated IGF-1 serum concentration unsupressible by oral glucose tolerance test (5). Based on the activity of acromegaly, the patient population was further divided. The activity of the disease was judged by an expert endocrinologist based on current guidelines: in those patients who had elevated serum hGH and IGF-1 concentration level above the diagnostic threshold and high IGF-1 index acromegaly was considered to be active. The present study is part of the MAGYAR-Path Study (Motion Analysis of the heart and Great vessels bY three-dimensionAl speckle-tRacking echocardiography in Pathological cases), which were created to assess diagnostic and prognostic value of 3DSTE-derived parameters ('magyar' means 'Hungarian' in Hungarian language). The MAGYAR-Path Study was approved by the human research committee of our institution and complied with the Declaration of Helsinki. All patients gave informed consent.

Two-dimensional doppler and tissue doppler echocardiography

Complete two-dimensional (2D) transthoracic echocardiography and 2D Doppler study were performed on all acromegaly patients and healthy controls using a Toshiba Artida™ imaging system (Toshiba Medical Systems, Tokyo, Japan) with a PST-30SBP (1–5 MHz) phased-array transducer. Chamber quantification and functional assessment were performed according to the current clinical standards (12).

Three-dimensional speckle-tracking echocardiography

3DSTE measurements were carried out using the same Toshiba Artida™ system with a PST-25SX matrix-array transducer (Toshiba Medical Systems, Tokyo, Japan). During a single breath-hold, six wedge-shaped subvolumes were obtained in the course of six constant RR intervals. These subvolumes were then automatically compiled into a pyramid-shaped full volume 3D dataset. To enhance spatial resolution and border detection all datasets were obtained in a focused view. Data analysis was performed offline using 3D Wall Motion Tracking software (version 2.7, Toshiba Medical Systems, Tokyo, Japan). The software automatically reconstructed the apical four-chamber (AP4CH) and two-chamber (AP2CH) views. Three cross-sectional planes then had to be specified by the reader using the software-supplied guide planes. After the planes were set up, the reader manually detected the right atrial (RA) endocardium using 6–8 datapoints from the lateral tricuspid annulus to the medial tricuspid annulus. The software using the specified planes and datapoints performed the speckle-tracking analysis on the 3D cast of the RA (7-10) (*Figure 1*).

3DSTE-derived RA volumetric- and functional parameters

3DSTE is capable of measuring numerous volumetric and functional RA parameters (*Figure 1*):
- End-systolic maximum RA volume (V_{max}, before tricuspid valve opening);
- RA volume before atrial contraction (V_{preA}, at the time of the P-wave on the ECG);
- End-diastolic minimum RA volume (V_{min}, before tricuspid valve closure).

The acquired volumetric data then can be used to calculate RA functional properties representing RA reservoir, conduit and active contraction functions (7-11):
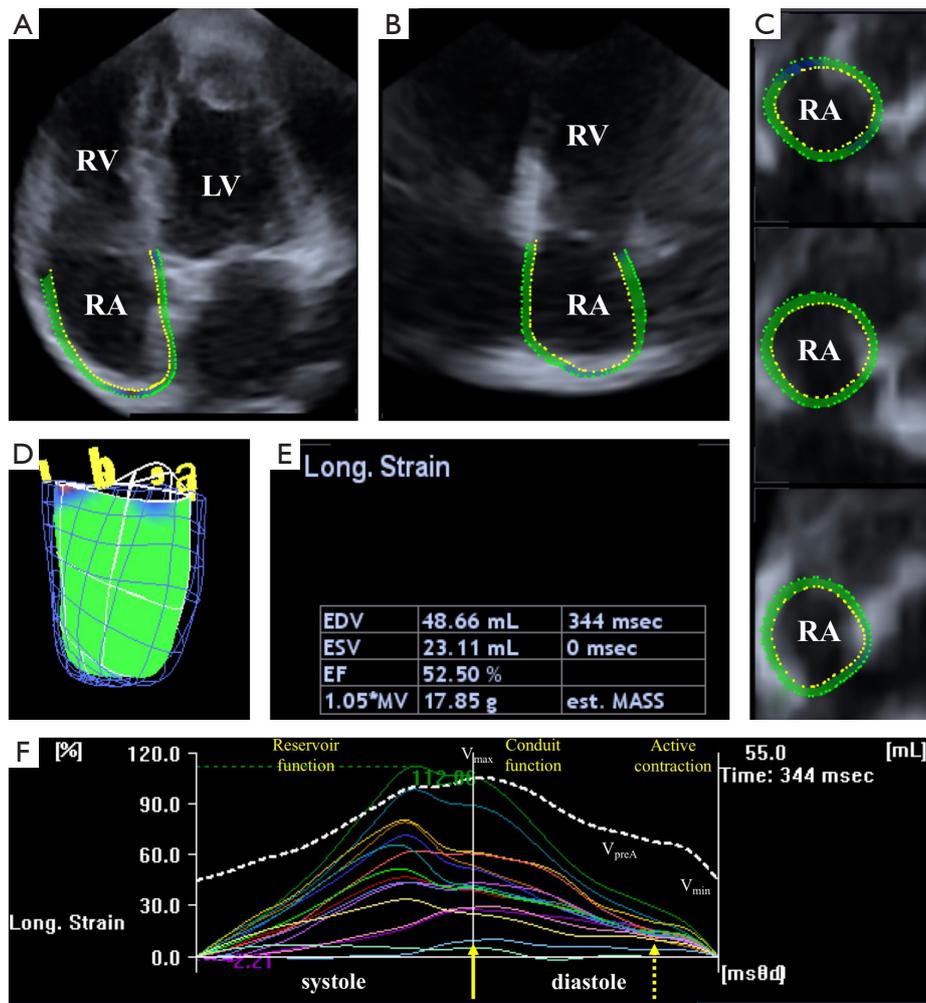
Reservoir function:
- Total stroke volume (SV) = $V_{max} - V_{min}$
- Total emptying fraction (EF) = Total SV/V_{max}

Conduit function:
- Passive SV = $V_{max} - V_{preA}$
- Passive EF = Passive SV/V_{max}

Active contraction:

Figure 1 Apical four-chamber (A) and two-chamber views (B) as well as short-axis views at the basal (C1), mid- (C2), and superior (C3) right atrial level derived from an active acromegaly patient's three-dimensional echocardiographic dataset. A three-dimensional cast of the right atrium (D) and corresponding volumetric data (E) during the cardiac cycle together with time-segmental strain curves of all right atrial segments and time–volume changes during the cardiac cycle (F) are also presented. The yellow arrow represents peak strain, while the dashed arrow represents strain at atrial contraction. Vmax, Vmin, and VpreA represent systolic maximum and diastolic minimum right atrial volumes and right atrial volume before atrial contraction, respectively. LV, left ventricle; RV, right ventricle; RA, right atrium.

- Active SV = $V_{preA} - V_{min}$
- Active EF = Active SV/V_{preA}

3DSTE-derived RA strain assessments

Using the same 3DSTE-derived RA model, the software is capable of obtaining several linear [radial (RS), longitudinal (LS) and circumferential (CS)] and complex [3D (3DS) and area (AS)] RA strains automatically. Based on the measurements not only regional strains were assessed but also global and mean segmental strains were calculated as

well. Peak RA strains were measured during RA reservoir phase at LV end-systole, and strains at atrial contraction were obtained during RA systole at LV end-diastole. Strains at atrial contraction represent RA booster pump function (*Figure 1*).

Statistical analysis

Datasets are reported as mean ± standard deviation. Confidence interval was chosen to be 95%, thus P values less than 0.05 were considered statistically significant. For assessment of normal distribution, Shapiro-Wilks test was

Table 1 Demographic clinical data and two-dimensional echocardiographic parameters of patients with acromegaly and controls

Data	Acromegaly patients (n=22)	Controls (n=44)	P value
Risk factors			
Age (years)	53.7±14.5	50.7±12.6	0.4
Male gender [%]	7 [33]	15 [34]	0.8
Hypertension [%]	11 [50]	11 [25]	0.06
Hypercholesterolemia [%]	9 [43]	8 [18]	0.07
Diabetes mellitus [%]	3 [14]	2 [5]	0.3
Medications			
β-blockers [%]	6 [29]	4 [9]	0.07
ACE-inhibitors [%]	7 [33]	6 [14]	0.1
ARB [%]	4 [19]	2 [5]	0.09
Diuretics [%]	7 [33]	5 [11]	0.09
Two-dimensional echocardiography			
LA diameter (mm)	42.4±6.6	37.9±4.4	0.009
LV end-diastolic diameter (mm)	50.6±4.3	48.0±3.6	0.03
LV end-diastolic volume (mL)	124.7±23.4	106.7±20.4	0.005
LV end-systolic diameter (mm)	30.2±4.5	31.5±2.9	0.1
LV end-systolic volume (mL)	38.2±12.7	36.9±8.9	0.7
Interventricular septum (mm)	10.5±1.6	9.5±1.4	0.03
LV posterior wall (mm)	10.8±1.7	9.6±1.7	0.008
LV ejection fraction (%)	68.8±7.5	65.1±3.7	0.049

LA, left atrium; LV, left ventricle; ACE, angiotensin-converting enzyme inhibitor; ARB, angiotensin II receptor blocker.

used. Levene's test was used to evaluate homogeneity of variances. Student's two-tailed *t*-test was used for normally distributed datasets, while Mann-Whitney Wilcoxon test was used for datasets not following a normal distribution. For the assessment of categorical variables Fisher's exact test was used. Pearson's correlation coefficients were calculated to establish significant correlation between independent variables. For offline data extraction and analysis, a commercial software package was used (MATLAB 8.6, The MathWorks Inc., Natick, MA, 2015). RStudio was used for all statistical calculations (RStudio Team, RStudio: Integrated Development for R. RStudio, Inc., Boston, MA, 2015).

Results

Clinical and demographic data of patients with acromegaly

The control group was risk factor-matched as well as age-

and gender-matched, therefore there were no significant differences between the acromegaly group and controls (*Table 1*). In the active acromegaly group 5 patients were on bromocriptine therapy and 4 patients were taking long-acting somatostatine analogues, also 6 patients had hypophysectomy previously. In the inactive acromegaly group 2 patients were taking bromocriptine, 3 patients were taking long-acting somatostatine analogues and 4 patients had successful hypophysectomy previously. In this group 2 patients required hormonal substitution therapy due to surgery: one patient was on hydrocortisone, desmopressin, L-thyroxine and estradiol, and the other patient was only on hydrocortisone and L-thyroxine.

Laboratory findings of patients with acromegaly

Active acromegaly group consisted of 10 patients (mean age:

Table 2 Comparison of 3DSTE-derived volumetric right atrial parameters of patients with acromegaly and controls

Data	Controls (n=44)	Acromegaly patients (n=22)	Active acromegaly patients (n=10)	Inactive acromegaly patients (n=12)
Calculated volumes (mL)				
V_{max}	47.2±13.5	54.5±14.4*	53.9±10.7	55.1±17.3
V_{min}	28.7±9.8	35.5±10.2*	36.0±9.2*	35.1±11.2
$V_{pre}A$	37.9±11.7	45.1±11.1*	45.7±8.5*	44.6±13.2
Stroke volumes (mL)				
TASV	18.5±8.9	19.0±8.1	17.8±4.7	19.9±10.3
PASV	9.3±6.4	9.4±6.2	8.2±4.7	10.4±7.3
AASV	9.2±5.3	9.6±4.8	9.6±3.6	9.5±5.8
Emptying fractions (%)				
TAEF	38.6±13.1	34.5±9.9	33.5±7.8	35.3±11.6
PAEF	19.3±10.7	16.7±8.8	14.9±7.0	18.2±10.1
AAEF	24.2±11.1	21.2±9.5	21.7±8.3	20.8±10.8

*, P<0.05 *vs.* controls; †, P<0.05 *vs.* active acromegaly group. V_{max}, maximum left atrial volume; V_{min}, minimum left atrial volume; V_{preA}, left atrial volume before atrial contraction; TASV, total atrial stroke volume; TAEF, total atrial emptying fraction; AASV, active atrial stroke volume; AAEF, active atrial emptying fraction; PASV, passive atrial stroke volume; PAEF, passive atrial emptying fraction.

58.3±12.4 years, 4 males). Their mean serum level of hGH was 5.5±4.0 ng/mL, IGF-1 level was 430.9 ±216.0 ng/mL and IGF-1 index was 1.8±1.0. In this group, hypophysectomy was performed in 6 cases (60%). The inactive disease group consisted of 12 patients (mean age: 49.9±15.5 years, 3 males). Their mean serum level of hGH was 5.2±8.2 ng/mL, IGF-1 level was 227.3±96.1 ng/mL and IGF-1 index was 1.2±1.1. In this group, hypophysectomy was performed in 4 cases (33%).

Two-dimensional echocardiographic data

Between the acromegaly group and healthy controls LA diameter (P=0.009), LV end-diastolic diameter (P=0.03) and volume (P=0.005) were significantly different. In case of acromegaly, both LV interventricular septum (P=0.03) and LV posterior wall (P=0.008) were significantly thicker compared to healthy controls and LV ejection fraction (P=0.049) was significantly higher in case of the acromegaly group as well (*Table 1*).

3DSTE-derived volumes and volume-based RA functional properties

All three RA volumetric parameters (Vmax, Vmin, VpreA) were significantly higher in case of acromegaly compared

to the healthy controls (P=0.03, P=0.009 and P=0.005, respectively). RA stroke volumes and emptying fractions were not significantly different compared to the control group. In case of active acromegaly, both Vmin (P=0.02) and VpreA (P=0.01) were significantly higher compared to the control group. In case of the other RA volume-derived functional properties, there was no significant difference between active disease and controls. The inactive disease group showed no significant difference compared to the healthy controls, also no significant differences could be detected between active and inactive acromegaly subgroups regarding RA volumetric and volume-based functional parameters (*Table 2*).

3DSTE-derived RA peak strain parameters

Both global and mean segmental 3DS were higher in the acromegaly group compared to the controls (P=0.03 and P=0.04, respectively), also mean segmental CS proved to be significantly lower in case of acromegaly (P=0.03). Out of the segmental strains, midatrial 3DS was significantly higher compared to the controls (P=0.04). Regarding global and mean segmental strains, the active acromegaly group showed significantly lower mean segmental LS (P=0.009) compared to the controls, moreover it is worthy to note

Table 3 Comparison of 3DSTE-derived global and mean segmental peak right atrial strain parameters in patients with acromegaly and controls

Data	Controls (n=44)	Acromegaly patients (n=22)	Active acromegaly patients (n=10)	Inactive acromegaly patients (n=12)
Global strains				
Radial (%)	−17.19±8.30	−20.07±8.36	−18.92±9.93	−21.03±7.10
Circumferential (%)	15.79±9.81	11.59±9.81	11.90±7.67	11.34±11.64
Longitudinal (%)	31.21±14.17	28.93±8.88	24.86±4.37	32.32±10.36
3D (%)	−7.88±4.80	−11.94±7.52*	−11.72±7.43	−12.13±7.91
Area (%)	49.43±27.05	38.99±16.30	37.18±13.44	40.50±18.82
Mean segmental strains				
Radial (%)	−21.45±7.44	−24.09±7.06	−23.69±8.14	−24.42±6.37
Circumferential (%)	22.14±10.61	16.77±9.45*	17.25±8.10	16.37±10.79
Longitudinal (%)	35.30±13.88	32.08±8.57	28.17±4.89*	35.34±9.75[†]
3D (%)	−13.61±5.08	−17.16±6.13*	−17.47±6.64	−16.91±5.96
Area (%)	58.58±29.13	46.21±15.51	43.88±14.67	48.15±16.56

*, P<0.05 *vs.* controls; [†], P<0.05 *vs.* active acromegaly group. 3D, three-dimensional.

that global and mean segmental 3DS were tendentiously higher, while global LS, global and mean segmental AS were tendentiously lower compared to the healthy controls. In the active acromegaly group there were no significant differences in case of peak regional RA strains compared to the control group. In the inactive acromegaly group, there were no significant differences compared to the controls regarding global and mean segmental RA peak strains, however global and mean segmental RS, and 3DS were tendentiously higher, where global and mean segmental AS were lower compared to the healthy controls. Midatrial 3DS (P=0.03) was significantly higher in the inactive acromegaly group as compared to the controls. Between the active and inactive group of acromegaly patients, mean segmental LS (P=0.04) was significantly different. Out of regional peak RA strains, midatrial LS (P=0.005) was significantly different between the acromegaly groups (*Tables 3,4*).

3DSTE-derived RA strain parameters at atrial contraction

At atrial contraction, mean segmental RS (P=0.04) and 3DS (P=0.04) were significantly higher in the acromegaly group compared to the controls. Superior and midatrial 3DS (P=0.049 and P=0.02, respectively) and midatrial RS (P=0.03) were significantly different out of the regional strains compared to the controls. In the active acromegaly subgroup, there were no significant differences regarding global and mean segmental strains compared to the healthy group. Out of the regional strains only the superior 3DS was significantly higher in the active acromegaly group compared to the controls (P=0.047). In the inactive acromegaly group, only midatrial 3DS was significantly higher as compared to the controls (P=0.027). The activity of acromegaly had no significant impact on RA strains at atrial contraction (*Tables 5,6*).

Correlation analysis

In the acromegaly group, no 2D or 3D echocardiography-derived parameter correlated significantly with hGH. 2D echocardiography-derived late transmitral flow velocity (A) (r=−0.454, P=0.04) and peak basal RS (r=−0.491, P=0.02) showed significant correlation with IGF-1 hormone levels in the acromegaly group. In this group, IGF-1 index correlated significantly with basal RS at atrial contraction (r=−0.569, P=0.007), superior RS at atrial contraction (r=−0.557, P=0.009), mean segmental RS at atrial contraction (r=−0.523, P=0.02), peak basal 3DS (r=−0.497, P=0.02), peak mean segmental 3DS (r=−0.443, P=0.04), basal 3DS at atrial contraction (r=−0.492, P=0.02), superior 3DS at atrial contraction (r=−0.502, P=0.02) and mean segmental 3DS at atrial contraction (r=−0.447, P=0.04). In the active acromegaly subgroup, hGH correlated significantly with peak basal LS (r=−0.683, P=0.03), peak

Table 4 Comparison of 3DSTE-derived regional peak right atrial strain parameters in patients with acromegaly and controls

Data	Controls (n=44)	Acromegaly patients (n=22)	Active acromegaly patients (n=10)	Inactive acromegaly patients (n=12)
RS_{basal} (%)	−20.66±7.74	−22.77±8.13	−25.36±8.99	−20.61±6.98
$RS_{midatrial}$ (%)	−20.66±9.26	−23.39±8.41	−21.27±8.55	−25.16±8.25
$RS_{superior}$ (%)	−23.79±12.89	−27.11±11.8	−24.80±13.30	−29.03±10.59
CS_{basal} %	24.21±13.79	17.85±8.98	18.39±9.46	17.41±8.96
$CS_{midatrial}$ (%)	19.25±9.05	15.18±8.95	15.53±7.79	14.88±10.15
$CS_{superior}$ (%)	23.11±20.29	17.54±17.38	18.12±13.51	17.06±20.66
LS_{basal} (%)	36.27±20.87	33.44±15.22	30.91±8.81	35.55±19.19
$LS_{midatrial}$ %	44.92±20.34	42.24±13.43	34.05±6.23	49.06±14.17[†]
$LS_{superior}$ (%)	19.40±11.33	14.80±9.92	15.23±9.39	14.44±10.74
$3DS_{basal}$ (%)	−13.16±5.89	−15.80±7.55	−17.88±7.31	−14.07±7.61
$3DS_{midatrial}$ (%)	−11.78±5.78	−15.39±5.31*	−14.58±5.82	−16.07±5.00*
$3DS_{superior}$ %	−17.04±10.59	−21.87±10.82	−21.20±12.22	−22.43±10.03
AS_{basal} (%)	53.99±38.30	42.92±19.07	44.91±19.27	41.26±19.59
$AS_{midatrial}$ (%)	67.88±32.08	56.50±19.12	48.29±14.78	63.33±20.17
$AS_{superior}$ (%)	51.54±47.45	35.71±36.72	35.72±28.54	35.71±43.67

*, P<0.05 *vs.* controls; [†], P<0.05 *vs.* active acromegaly group. RS, radial strain; CS, circumferential strain; LS, longitudinal strain; 3DS, three-dimensional strain; AS, area strain.

Table 5 Comparison of 3DSTE-derived global and mean segmental right atrial strain parameters at atrial contraction in patients with acromegaly and controls

Data	Controls (n=44)	Acromegaly patients (n=22)	Active acromegaly patients (n=10)	Inactive acromegaly patients (n=12)
Global strains				
Radial (%)	−7.34±6.11	−10.60±8.15	−12.44±9.08	−9.07±7.33
Circumferential (%)	10.24±9.05	6.44±7.44	7.34±7.31	5.70±7.79
Longitudinal (%)	7.59±6.45	8.44±5.82	10.05±6.78	7.09±4.76
3D (%)	−4.00±3.76	−6.40±7.10	−8.11±7.62	−4.97±6.61
Area (%)	18.11±17.29	18.73±17.69	21.01±18.67	16.83±17.43
Mean segmental strains				
Radial (%)	−9.65±4.41	−13.22±6.45*	−14.74±7.25	−11.96±5.71
Circumferential (%)	11.15±7.41	9.08±6.18	10.36±6.50	8.01±5.96
Longitudinal (%)	10.63±5.81	11.35±5.13	13.52±6.30	9.55±3.15
3D (%)	−6.70±3.58	−9.78±5.44*	−10.74±5.68	−8.98±5.35
Area (%)	21.73±13.83	22.19±12.47	25.27±14.80	99.62±10.10

*, P<0.05 *vs.* controls. 3D, three-dimensional.

Table 6 Comparison of 3DSTE-derived regional right atrial strain parameters at atrial contraction in patients with acromegaly and controls

Data	Controls (n=44)	Acromegaly patients (n=22)	Active acromegaly patients (n=10)	Inactive acromegaly patients (n=12)
RS_{basal} (%)	−10.25±5.59	−13.14±7.20	−15.87 ±7.71	−10.86±6.15
$RS_{midatrial}$ (%)	−8.87±4.95	−12.57±6.99*	−13.07±7.62	−12.16±6.74
$RS_{superior}$ (%)	−9.93±7.52	−14.32±9.02	−15.55±11.07	−13.30±7.25
CS_{basal} %)	12.11±8.20	9.19±7.44	9.88±6.82	8.61±8.17
$CS_{midatrial}$ (%)	10.22±6.96	8.15±5.14	8.83±5.82	7.58±4.70
$CS_{superior}$ (%)	10.07±11.11	10.31±11.53	13.39±11.95	7.73±11.01
LS_{basal} (%)	10.73±7.09	9.85±6.02	12.42±6.88	7.70±4.42
$LS_{midatrial}$ %)	12.04±6.95	14.85±7.56	16.85±9.11	13.18±5.86
$LS_{superior}$ (%)	8.41±8.64	8.36±6.99	10.16±7.61	6.87±6.38
$3DS_{basal}$ (%)	−6.85±4.85	−8.56±5.62	−10.30±5.49	−7.11±5.53
$3DS_{midatrial}$ (%)	−5.81±3.70	−9.20±5.95*	−9.22±6.61	−9.19±5.64*
$3DS_{superior}$ %)	−7.80±7.06	−12.47±8.07*	−13.68±9.17*	−11.46±7.28
AS_{basal} (%)	21.08±11.99	18.50±12.25	23.33±15.52	14.49±7.11
$AS_{midatrial}$ (%)	22.42±14.10	27.01±13.15	27.30±13.52	26.76±13.42
$AS_{superior}$ (%)	21.65±26.05	20.48±24.04	25.15±24.32	16.59±24.14

*, $P<0.05$ vs. controls. RS, radial strain; CS, circumferential strain; LS, longitudinal strain; 3DS, three-dimensional strain; AS, area strain.

global LS (r=−0.690, P=0.03) and global LS at atrial contraction (r=−0.656, P=0.04). IGF-1 hormone levels in the active acromegaly group correlated significantly with peak basal RS (r=−0.707, P=0.04), mean segmental basal RS (r=−0.654, P=0.04), basal RS at atrial contraction (r=−0.654, P=0.04), superior RS at atrial contraction (r=−0.654, P=0.04), global RS at atrial contraction (r=−0.732, P=0.02), mean segmental RS at atrial contraction (r=−0.741, P=0.01), peak midatrial CS (r=0.680, P=0.03), peak global CS (r=0.672, P=0.03), peak mean segmental CS (r=0.638, P=0.047), basal CS at atrial contraction (r=0.643, P=0.045), midatrial CS at atrial contraction (r=0.819, P=0.004), global CS at atrial contraction (r=0.705, P=0.02), mean segmental CS at atrial contraction (r=0.713, P=0.02), global LS at atrial contraction (r=0.722, P=0.02), superior 3DS at atrial contraction (r=−0.651, P=0.04), peak basal AS (r=0.687, P=0.03), peak mean segmental AS (r=0.690, P=0.03), basal AS at atrial contraction (r=0.784, P=0.007), midatrial AS at atrial contraction (r=0.650, P=0.04) and mean segmental AS at atrial contraction (r=0.738, P=0.02). IGF-1 index correlated significantly in the active disease group with peak basal RS (r=−0.648, P=0.04), peak mean segmental RS

(r=−0.671, P=0.03), basal RS at atrial contraction (r=−0.635, P=0.049), midatrial RS at atrial contraction (r=−0.642, P=0.045), superior RS at atrial contraction (r=−0.712, P=0.02), global RS at atrial contraction (r=−0.801, P=0.005), mean segmental RS at atrial contraction (r=−0.778, P=0.008), peak midatrial CS (r=0.672, P=0.03), peak global CS (r=0.643, P=0.045), midatrial CS at atrial contraction (r=0.795, P=0.006), mean segmental CS at atrial contraction (r=0.675, P=0.03), basal LS at atrial contraction (r=0.634, P=0.049), global LS at atrial contraction (r=0.743, P=0.01), superior 3DS at atrial strain (r=−0.711, P=0.021), mean segmental 3DS at atrial contraction (r=-0.633, P=0.049), peak basal AS (r=0.666, P=0.04), peak mean segmental AS (r=0.666, P=0.04), basal AS at atrial contraction (r=0.775, P=0.009) and mean segmental AS at atrial contraction (r=0.686, P=0.03). In the inactive acromegaly group, hGH had no significant correlation with any independent variables. In this group, IGF-1 correlated significantly with 2D LV ESD (r=0.657, P=0.03) and 2D LV ESV (r=0.675, P=0.02). In the inactive disease group, IGF-1 index correlated significantly with 2D LV ESD (r=0.645, P=0.03) and 2D LV ESV (r=0.660, P=0.03).

Discussion

Acromegaly is a relatively rare, hormonal, chronic disease involving several organs through elevated hGH and IGF-1 levels (13). Cardiovascular involvement is especially common in acromegalic patients, from the most common hypertension to cardiomyopathy (14). Pathophysiology of these cardiac co-morbidities is not clearly understood, although studies show that acromegaly entails a specific type of cardiomyopathy, which might result in severe heart failure at end-stages. In the early stages of the disease, LV hypertrophy develops due to hyperkinetic syndrome and as the disease progresses, collagen deposition begins. This extracellular collagen causes at first diastolic and later systolic heart failure. At end-stages, congestive heart failure develops combined with valvular insufficiencies and increased incidence of arrhythmias (atrial fibrillation is the most common). The hyperkinetic syndrome is caused by hGH and IGF-1 mediated Ca^{2+} hypersensitivity and reduced peripheral vascular resistance at the beginning (15-21). Furthermore, elevated hormone levels cause sodium retention and subsequent plasma expansion resulting in circulatory volume increase (22-24). To the best of the author's knowledge there are no 3DSTE studies examining the effect of acromegaly treatment on RA function, however Heidarpour *et al.* recently published a systematic review on the effect of somatostatin analog treatment on cardiovascular parameters in acromegaly. According to this study heart rate and left ventricular mass index decreased significantly after treatment, and E/A ratio improved significantly in a few studies, as well (25).

There are emerging, new echocardiographic techniques such as 3D echocardiography and/or STE. These modalities are capable of not only assessing the LV but also the atria using a "block-matching" by strain analysis algorithm. Volumetric real-time 3D echocardiography (RT3DE) is widely regarded as a non-invasive, accurate tool for the volumetric and volume-derived functional assessment of the atria (7-10). In previous studies, 3DSTE was found to be comparable and interchangeable to RT3DE (26). Our group has also demonstrated that 3DSTE is a feasible tool in volumetric and strain imaging of RA previously (7-10).

RA has a distinct phasing function throughout the cardiac cycle. During RV systole, it functions as a reservoir, during early RV diastole, RA conducts the blood from the caval veins to the RV, and lastly in late RV diastole, RA contractions act as a booster pump to RV filling (11). Total, passive and active SVs and EFs correspond to these phasic functions. The complete 3DSTE datasets gave us the possibility to not only characterize RA function by volume and volume-derived functional parameters but to assess global, mean segmental and regional peak strains and strains at atrial contraction at the same time, as well.

To the best of the author's knowledge, there are no studies characterizing RA volumes, volume-based functional properties and strains at the same time in acromegaly patients using 3DSTE. However, our group previously demonstrated that aortic stiffness is increased in acromegaly (27) with its prognostic value (28). LV twist was found to be impaired in acromegaly regardless of disease activity (29) and most importantly, LA function was found to be similarly enhanced in case of active acromegaly (30).

The data presented in this study suggests profound RA remodellation, especially in active acromegaly as compared to the healthy group. Furthermore, strain analysis revealed that RA function may be enhanced in acromegalic patients, which is more notable in case of active disease. Correlation analysis revealed that numerous independent strain parameters had significant correlations with different hormonal variables in the active acromegaly group. These correlations were not present in the inactive acromegaly subgroup however. These results suggest that RA remodellation and functional changes may subside with proper treatment of the disease. These changes may be reactive to the LV and LA dysfunction that are characteristic in acromegaly. However, collagen deposition cannot be ruled out as it affects the whole heart not only the LV, thus causing parallel RA remodellation as well, similarly to LA and LV remodellation. The real mechanism involved is not completely understood yet at present, however RV remodellation might have a direct effect on RA changes. As of yet there are no studies characterizing RV changes in acromegaly or confirming whether RV behaves in the same manner as LV in this disease, thus resulting in impaired RV filling entailing RA enlargement and subsequent remodellation. These questions warrant further studies in this field.

Limitations

There are numerous limiting factors of the present study, mainly the relatively low number of patients involved. The duration of acromegaly/inactivity of acromegaly or the effect of drugs were not investigated. Currently there are no reference values for RA strains, therefore the reported strains of our control group might differ compared to other

articles. There are several technical limiting factors as well, such as the relatively low spatial and temporal resolution of current 3DSTE methodologies. Full volume datasets are acquired through 6 RR intervals and this might cause so called "stitching noise" (31).

Conclusions

Acromegaly has a profound effect on RA function and with proper treatment, these changes partly seem to be reversible.

Acknowledgments

Footnote

Conflicts of Interest: AN serves as an unpaid editorial board member of Quantitative Imaging in Medicine and Surgery. The other authors have no conflicts of interest to declare.

References

1. Sanno N, Teramoto A, Osamura RY, Horvath E, Kovacs K, Lloyd RV, Scheithauer BW. Pathology of pituitary tumors. Neurosurg Clin N Am 2003;14:25-39, vi.
2. Colao A, Ferone D, Marzullo P, Lombardi G. Systemic complications of acromegaly: epidemiology, pathogenesis, and management. Endocr Rev 2004;25:102-52.
3. Clayton RN. Cardiovascular function in acromegaly. Endocr Rev 2003;24:272-7.
4. Ramos-Leví AM, Marazuela M. Cardiovascular comorbidities in acromegaly: an update on their diagnosis and management. Endocrine 2017;55:346-59.
5. Melmed S. Medical progress: Acromegaly. N Engl J Med 2006;355:2558-73.
6. Seo Y, Ishizu T, Atsumi A, Kawamura R, Aonuma K. Three-dimensional speckle tracking echocardiography. Circ J 2014;78:1290-301.
7. Piros GÁ, Domsik P, Kalapos A, Lengyel C, Orosz A, Forster T, Nemes A. Relationships between right atrial and left ventricular size and function in health subjects. Results from the three-dimensional speckle-tracking echocardiographic MAGYAR-Healthy Study. Orv Hetil 2015;156:972-8.
8. Nemes A, Földeák D, Domsik P, Kalapos A, Kormányos Á, Borbényi Z, Forster T. Right Atrial Deformation Analysis in Cardiac Amyloidosis - Results from the Three-Dimensional Speckle-Tracking Echocardiographic MAGYAR-Path Study. Arq Bras Cardiol 2018;111:384-91.
9. Nemes A, Domsik P, Kalapos A, Gavaller H, Oszlanczi M, Forster T. Right atrial deformation analysis in isolated left ventricular noncompaction - insights from the three-dimensional speckle tracking echocardiographic MAGYAR-Path Study. Rev Port Cardiol 2016;35:515-21.
10. Nemes A, Havasi K, Domsik P, Kalapos A, Forster T. Evaluation of right atrial dysfunction in patients with corrected tetralogy of Fallot using 3D speckle-tracking echocardiography. Insights from the CSONGRAD Registry and MAGYAR-Path Study. Herz 2015;40:980-8.
11. Rai AB, Lima E, Munir F, Faisal Khan A, Waqas A, Bughio S, ul Haq E, Attique HB, Rahman ZU. Speckle Tracking Echocardiography of the Right Atrium: The Neglected Chamber. Clin Cardiol 2015;38:692-7.
12. Lang RM, Badano LP, Mor-Avi V, Afilalo J, Armstrong A, Ernande L, Flachskampf FA, Foster E, Goldstein SA, Kuznetsova T, Lancellotti P, Muraru D, Picard MH, Rietzschel ER, Rudski L, Spencer KT, Tsang W, Voigt JU. Recommendations for cardiac chamber quantification by echocardiography in adults: an update from the American Society of Echocardiography and the European Association of Cardiovascular Imaging. Eur Heart J Cardiovasc Imaging 2015;16:233-70.
13. Frara S, Maffezzoni F, Mazziotti G, Giustina A. The Modern Criteria for Medical Management of Acromegaly. Prog Mol Biol Transl Sci 2016;138:63-83.
14. Dineen R, Stewart PM, Sherlock M. Acromegaly. QJM 2017;110:411-20.
15. dos Santos Silva CM, Gottlieb I, Volschan I, Kasuki L, Warszawski L, Balarini Lima GA, Xavier SS, Pedrosa RC, Neto LV, Gadelha MR. Low Frequency of Cardiomyopathy Using Cardiac Magnetic Resonance Imaging in an Acromegaly Contemporary Cohort. J Clin Endocrinol Metab 2015;100:4447-55.
16. Colao A, Marzullo P, Di Somma C, Lombardi G.

Growth hormone and the heart. Clin Endocrinol (Oxf) 2001;54:137-54.

17. Bogazzi F, Lombardi M, Strata E, Aquaro G, Di Bello V, Cosci C, Sardella C, Talini E, Martino E. High prevalence of cardiac hypertophy without detectable signs of fibrosis in patients with untreated active acromegaly: an in vivo study using magnetic resonance imaging. Clin Endocrinol (Oxf) 2008;68:361-8.

18. Saccà L, Napoli R, Cittadini A. Growth hormone, acromegaly, and heart failure: an intricate triangulation. Clin Endocrinol (Oxf) 2003;59:660-71.

19. Powlson AS, Gurnell M. Cardiovascular Disease and Sleep-Disordered Breathing in Acromegaly. Neuroendocrinology 2016;103:75-85.

20. Pereira AM, van Thiel SW, Lindner JR, Roelfsema F, van der Wall EE, Morreau H, Smit JW, Romijn JA, Bax JJ. Increased prevalence of regurgitant valvular heart disease in acromegaly. J Clin Endocrinol Metab 2004;89:71-5.

21. Kahaly G, Olshausen KV, Mohr-Kahaly S, Erbel R, Boor S, Beyer J, Meyer J. Arrhythmia profile in acromegaly. Eur Heart J 1992;13:51-6.

22. Vitale G, Pivonello R, Auriemma RS, Guerra E, Milone F, Savastano S, Lombardi G, Colao A. Hypertension in acromegaly and in the normal population: prevalence and determinants. Clin Endocrinol (Oxf) 2005;63:470-6.

23. Bondanelli M, Ambrosio MR, degli Uberti EC. Pathogenesis and prevalence of hypertension in acromegaly. Pituitary 2001;4:239-49.

24. Brevetti G, Marzullo P, Silvestro A, Pivonello R, Oliva G, di Somma C, Lombardi G, Colao A. Early vascular alterations in acromegaly. J Clin Endocrinol Metab 2002;87:3174-9.

25. Heidarpour M, Shafie D, Aminorroaya A, Sarrafzadegan N, Farajzadegan Z, Nouri R, Najimi A, Dimopolou C, Stalla G. Effects of somatostatin analog treatment on cardiovascular parameters in patients with acromegaly: A systematic review. J Res Med Sci 2019;24:29.

26. Kleijn SA, Brouwer WP, Aly MF, Rüssel IK, de Roest GJ, Beek AM, van Rossum AC, Kamp O. Comparison between three-dimensional speckle-tracking echocardiography and cardiac magnetic resonance imaging for quantification of left ventricular volumes and function. Eur Heart J Cardiovasc Imaging 2012;13:834-9.

27. Nemes A, Gavaller H, Csajbok E, Julesz J, Forster T, Csanady M. Aortic stiffness is increased in acromegaly--a transthoracic echocardiographic study. Int J Cardiol 2008;124:121-3.

28. Csajbók E, Kalapos A, Gavallér H, Wittmann T, Csanády M, Forster T, Nemes A. Prognostic significance of aortic stiffness index in acromegaly--results from a 4-year follow-up. Int J Cardiol 2011;147:457-9.

29. Kormányos Á, Domsik P, Kalapos A, Orosz A, Lengyel C, Valkusz Z, Trencsányi A, Forster T, Nemes A. Left ventricular twist is impaired in acromegaly: Insights from the three-dimensional speckle tracking echocardiographic MAGYAR-Path Study. J Clin Ultrasound 2018;46:122-8.

30. Kormányos Á, Domsik P, Kalapos A, Valkusz Z, Lengyel C, Forster T, Nemes A. Three-dimensional speckle tracking echocardiography-derived left atrial deformation analysis in acromegaly (Results from the MAGYAR-Path Study). Echocardiography 2018;35:975-84.

31. Seo Y, Ishizu T, Aonuma K. Current status of 3-dimensional speckle tracking echocardiography: a review from our experiences. J Cardiovasc Ultrasound 2014;22:49-57.